

AD-A089 528

MICHIGAN TECHNOLOGICAL UNIV HOUGHTON DEPT OF METALLU--ETC F/6 20/11  
CRACK PROPAGATION ALONG CRYSTALLOGRAPHIC SLIP BANDS AND HYDROGE--ETC(U)  
AUG 80 J R WILCOX, D A KOSS N00014-76-C-0037  
TR-14 NL

UNCLASSIFIED

1 of 1  
AD-A089 528



END  
DATE  
FILMED  
10-80  
DTIC

**LEVEL**

(12)

TECHNICAL REPORT No. 14

To

THE OFFICE OF NAVAL RESEARCH  
CONTRACT No. N00014-76-C-0037

AD A 089528

CRACK PROPAGATION ALONG CRYSTALLOGRAPHIC  
SLIP BANDS AND HYDROGEN EMBRITTLEMENT

By

J. R. WILCOX AND D. A. KOSS

DEPARTMENT OF METALLURGICAL ENGINEERING  
MICHIGAN TECHNOLOGICAL UNIVERSITY  
HOUGHTON, MICHIGAN U.S.A.

DTIC  
SELECTED  
SEP 26 1980

A

REPRODUCTION IN WHOLE OR IN PART IS PERMITTED FOR ANY PURPOSE  
OF THE UNITED STATES GOVERNMENT. DISTRIBUTION OF THIS DOCUMENT  
IS UNLIMITED.

80 9 25 018

DC FILE COPY

To be presented at the Third International Conference on Effect of Hydrogen on Behavior of Materials, Jackson Lake Lodge, Wyoming, August 26-31, 1980.

CRACK PROPAGATION ALONG CRYSTALLOGRAPHIC SLIP BANDS  
AND HYDROGEN EMBRITTLEMENT

J. R. Wilcox<sup>†</sup> and D. A. Koss

Department of Metallurgical Engineering  
Michigan Technological University  
Houghton, MI 49931

The propagation of an inclined crack along a coplanar slip band is examined with regard to the conditions usually associated with hydrogen embrittlement. The analysis shows that large normal stresses are located very near to the crack-tip, despite the mixed mode nature of such cracks. This state of stress, the presence of the planar slip at the crack-tip, and a small but probably significant amount of non-coplanar slip all contribute to a set of conditions which are very favorable to hydrogen embrittlement. In view of the analysis, the effect of gaseous environment on the fatigue crack propagation behavior of an age hardenable metastable  $\beta$ -phase Ti-30V alloy has been examined. Tests on both single crystal and polycrystalline specimens show that, consistent with the analysis, gaseous hydrogen accelerates the fatigue crack growth rates only when Stage I fatigue occurs along a crystallographic {112} slip plane.

Accession For	
NTIS Grant	<input checked="" type="checkbox"/>
Doc. No.	
Unannounced	
Availability	
Project	
Institution	
Applicant's Address	
Dist	Available or special
A	

<sup>†</sup>Presently at: General Electric Co., Research and Development Center, Schenectady, NY 12345

### Introduction

The propagation of a crack along a crystallographic slip band occurs frequently in alloys susceptible to planar, non-uniform slip. Such crystallographic cracking occurs in large grain or single crystal material and on planes inclined to the stress axis and is most commonly observed under cyclic loading conditions in high strength Ni-, Al-, and Ti alloys. In all of these materials, cracks propagating along slip bands usually have a substantially brittle or cleavage-like fracture appearance, which can be sensitive to the environment.<sup>1-4</sup> This suggests that normal stresses and environmental effects are important in this fracture process.

Certain conditions for the propagation of a crack along a coplanar slip band (i.e., the slip plane and the slip vector are parallel to the plane of the crack, although not necessarily in the crack plane) have been analyzed by Koss and Chan.<sup>5,6</sup> In their model, a relaxed "elastic-plastic" state of stress exists ahead of a crack propagating along a slip band. Calculations show that this stress state is not conducive for activating secondary slip with a Burger's vector inclined to the crack plane.<sup>5</sup> As a result, large normal stresses can be generated near the tip of an inclined, mixed-mode crack propagating along a crystallographic slip band, particularly for basal plane cracking in an hcp material.<sup>6</sup> The purpose of this paper is to examine crack propagation along coplanar slip bands with regard to the conditions favoring hydrogen embrittlement. We will also show that, consistent with the model, an alloy (bcc Ti-30V, in this case) can be susceptible to hydrogen-assisted cracking if it is heat-treated to promote crack propagation along crystallographic slip bands.

### Crack Propagation Along Planar Slip Bands and the Resulting Stress Stage

The basis for understanding crack propagation along a coplanar slip band is contained in Fig. 1 and is discussed in more detail by Koss and Chan.<sup>5,6</sup> If the crack-tip plasticity is dominated by coplanar slip whose Burger's vector is also coplanar with the crack, then the planar slip plastic zone extends to distance  $r_p$  ahead of the crack-tip. The singularity in the elastic stress field near the tip of a mixed mode crack dictates that if  $r$  is the radial distance from the crack-tip, then  $\sigma_{ij} \propto 1/\sqrt{r}$ , where  $\sigma_{ij}$  is a stress component. A key feature shown in Fig. 1 is the recognition that coplanar slip relaxes the shear stresses  $\sigma_{xy}$  and  $\sigma_{yz}$  to values ( $\sigma_{xy}^*$  and  $\sigma_{yz}^*$ ) roughly determined by critical resolved yield stress  $\tau_y$  of the material since  $\tau_y = \sigma_{xy}^* \sin\phi + \sigma_{yz}^* \cos\phi$  at  $r \leq r_p$ .<sup>†</sup> However, the coplanar slip and the resulting relaxation of the shear stresses (the associated displacements are akin to sliding a deck of cards) does not produce displacements which are dilatational. Thus, the normal stress components  $\sigma_{ii}$  continue to increase until very close to the crack-tip when at  $r = r_p$ , non-coplanar slip is activated. This is shown in Fig. 1. It is important to realize that this relaxed,

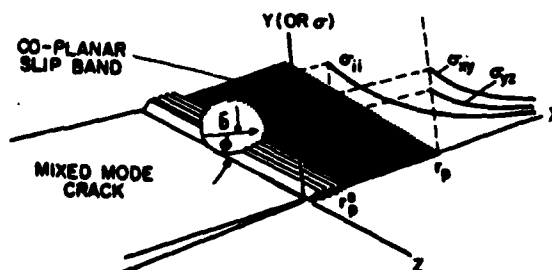


Fig. 1. A schematic illustration of the stress state ahead of a mixed mode crack with a coplanar slip band characterized by a slip vector  $b$  at angle  $\phi$  to the crack front. The coplanar slip extends to  $r_p$  which non-coplanar slip is activated to  $r_p^*$  (after Koss and Chan).

†Note that in the plane of a crack,  $\sigma_{xz} = 0$  and that  $\phi$  is the angle between the crack front ( $z$  axis) and the slip vector of the coplanar slip band.

elastic-plastic stress state is not conducive for activation of non-coplanar slip (i.e., in plane strain, the normal stresses are nearly balanced triaxial;  $\sigma_{xx} = \sigma_{yy} = 3/2 \sigma_{zz}$ ). However, this stress state is well-suited for the development of large normal stresses near the crack-tip.

Ignoring plastic relaxation, crack-tip blunting, work hardening effects, and assuming the normal stresses to obey the same functional dependence on  $r$  and elastic stress intensity factor regardless of any relaxation of  $\sigma_{xy}$  and  $\sigma_{yz}$ , Koss and Chan have estimated the magnitude of the maximum normal stresses for three different crack orientations and for fcc, hcp, and bcc slip crystallography.<sup>6</sup> Those calculations show that for 45° inclined, mixed-mode cracks, the maximum value of the hydrostatic stress  $\sigma_H^m$  is much greater for crack propagation along a slip band than if multiple slip occurred ahead of the crack.

The effect of the crystallography of slip in fcc, hcp, and bcc alloys on  $\sigma_H^m$  has also been examined.<sup>6</sup> As might be expected, very large hydrostatic stresses are predicted to be present near the tip of a crack propagating along a basal plane in an hcp crystal. This is due to the difficulty of activating slip or twinning which causes an extension (or relaxation of the normal stresses) in the C direction, normal to the (0001) plane. Extension along the C axis by twinning on the  $\{10\bar{1}2\} \langle \bar{1}101 \rangle$  system, which is very common to most hcp alloys, is probably the most likely means that hcp metals have of relaxing the large normal stresses near the crack-tip. Observations of Stage I fatigue along the basal plane in hcp Ti alloys show that  $\{10\bar{1}2\}$  twins are indeed found near the tip of crystallographic cracks.<sup>7,8</sup> Another interesting result is that, despite many available secondary slip systems, relatively large hydrostatic stresses can also be generated by crystallographic slip band cracking in both fcc and bcc material.<sup>6</sup> An implication of these calculations is that a cubic alloy might be sensitive to hydrogen embrittlement effects if it is heat-treated to promote planar slip and crack propagation occurs along a coplanar slip band (assuming that the kinetics of hydrogen transport are sufficiently rapid).

#### The Maximum Stress Location $x_m$

The position  $x_m$  of the maximum hydrostatic stress ahead of a crack-tip is important in hydrogen embrittlement because it will influence the time scale that H must diffuse (or be swept in). The methodology used in the above calculations assumes that the maximum normal stresses occur near the elastic-plastic interface for non-coplanar slip (i.e., at  $r = r_p^s$ ). While crude, this method yields a value for a mode I crack which agrees well with continuum plasticity estimates for a von Mises material.<sup>9</sup> However, the continuum plasticity estimates based on multiple slip and a mode I crack place the largest value of the maximum principal stress at a distance  $x_m$  being two times the crack-tip opening displacement between the upper and lower crack faces.<sup>9</sup> In the absence of detailed continuum plasticity calculations in the present case, it is reasonable to conclude that the maximum stress position  $x_m$  for this form of crystallographic cracking is:

$$2\delta \lesssim x_m \lesssim r_p^s \quad (1)$$

where  $\delta$  is the normal component of the crack-tip opening displacement for a mixed-mode crack and therefore is related to the extent of non-coplanar slip. Physically Eq. (1) implies that as one approaches the crack-tip in a non-hardening material, the normal stresses  $\sigma_{ii}$  in Fig. 1 are constant

within the coplanar plastic zone from  $x = r_p^s$  to  $x = 2\delta$  at which point the stresses begin to relax due to the surfaces of the crack.

The important feature to recognize in this analysis is that Eq. (1) places the maximum normal stresses very near the crack-tip and thus results in relatively short H diffusion/sweep in distances. The values of  $r_p$ ,  $r_p^s$ , and therefore  $x_m$  for a given crack geometry and crystal system can be calculated using the method outlined in the Appendix of Ref. 6. For example, in the case of a mixed mode I/II crack inclined  $45^\circ$  across the width of a plate in plane strain,  $x_m \leq .07 r_p$  for an fcc crystal cracking along a  $\{111\}$  plane, and  $x_m \leq .02 r_p$  for an hcp crystal with a basal crack. The crack-tip opening displacement criteria would result in an even smaller value of  $x_m$ . A rigorous calculation of  $\delta$  is beyond the scope of this paper; it would involve knowing the detailed shape of the secondary slip plastic zone which in turn requires an accurate knowledge of radial distribution of stresses for the stress state shown schematically in the plane of the crack at  $\theta = 0^\circ$  in Fig. 1. An estimate of  $\delta$  can be made by assuming  $r_p^s \neq f(\theta)$ , in which case  $\delta \approx 2(\tau_y/\mu)r_p^s \int_0^\pi \sin\theta d\theta = 4(\tau_y/\mu)r_p^s$ , where  $\mu$  is the shear modulus. Given that  $\tau_y/\mu \approx 10^{-2}$  for a high strength alloy, Eq. (1) becomes:  $10^{-1} r_p^s \leq x_m \leq r_p^s$ . In view of the magnitude of  $r_p^s$ , this places  $x_m$  very close to the crack-tip, minimizing the diffusion/sweep in distance of an external hydrogen source.

In summary, the large normal stresses, the presence of planar slip which enhances any film rupture and hydrogen sweep in process, and the location of the maximum stress being near the crack-tip are all conditions which favor hydrogen embrittlement phenomena, especially due to external hydrogen. It is also likely that the small amount of non-coplanar slip present near the crack-tip is important in providing sufficient crack opening separation of the upper and lower crack surfaces to allow an environmental interaction and to hinder slip reversibility within the planar slip band. All of the above suggests that an alloy which might be otherwise immune to hydrogen embrittlement may become susceptible to hydrogen-assisted cracking if it is heat treated so that cracking along a crystallographic slip band occurs.

#### Hydrogen-Assisted Fatigue Crack Propagation in a Beta Titanium Alloy

In view of the above analysis, the effect of a gaseous environment on the fatigue crack propagation behavior of an age hardenable, metastable  $\beta$ -phase (bcc) Ti-30V alloy has been examined. Beta Ti alloys are usually considered to be immune to hydrogen embrittlement effects.<sup>10</sup> However, the Ti-30V alloy can be heat-treated in the temperature range of  $300^\circ\text{C}$  to precipitate very fine, coherent  $\omega$ -phase particles. Such precipitation is known to result in a transition from fine, wavy slip in the solution-treated condition to planar, non-uniform slip after age hardening by the  $\omega$ -phase particles.<sup>11</sup> In fatigue, the precipitation of the  $\omega$ -phase can also cause a transition in the plane of fatigue crack propagation. Stage II fatigue (i.e., propagation involving multiple slip and on a plane normal to the stress axis) dominates Ti-27V solution-treated material while Stage I fatigue (crack propagation along a crystallographic slip plane inclined to the stress axis) frequently occurs in the  $\omega$ -phase hardened condition.<sup>12</sup> This study utilizes the age hardening behavior of the Ti-30V alloy and the use of single crystal specimens to examine the influence of gaseous hydrogen on both Stage I and Stage II fatigue behavior.

Polycrystalline samples with an average grain size of 0.057 mm and seeded single crystals in the form of identical strips  $\sim 1.5$  mm thick were tested. The configuration of the test samples consisted of a gauge length

25.4 mm long x 6.35 mm wide with a centrally located hole which acted as a crack starter. The orientation of the single crystal samples is shown in Fig. 2 and was chosen so that crack propagation along the most highly stressed  $\{211\}$  slip plane should result in a mixed mode I/II crack inclined across the width of the sample. This crystal orientation makes through-thickness slip very difficult and assures predominantly plane strain at small stress intensity levels even with the relatively thin samples. Plane strain also dominates the polycrystalline samples at least to stress intensity ranges up to  $\Delta K = 20 \text{ MPa}\sqrt{\text{m}}$ ; this is based on cyclic plastic zone size calculations ( $r_p < .04 \times \text{thickness}$ ) and visual observations. Prior to testing, all of the samples were He gas quenched from  $800^\circ\text{C}$ , and the single crystals were age hardened at  $300^\circ\text{C}$  for 53 hours, which increased the hardness from 230 DPH to 350-380 DPH. The Ti-30 at.% V (31.5 wt.%) single crystal samples contained (in wt. ppm): 950 O, 41 H, 260 N, and 240 C while the polycrystalline specimens contained: 720 O, 31 H, 320 N, and 190 C.

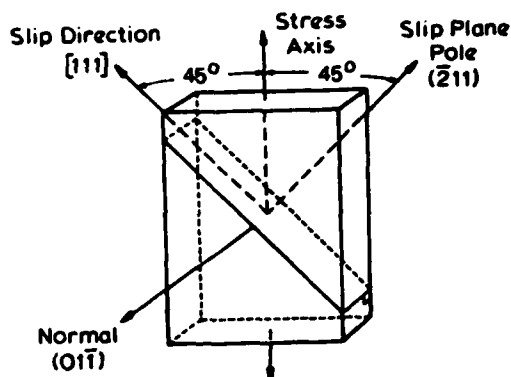


Fig. 2. The orientation of the single crystal specimens examined in this study.

Fatigue testing was performed at 30 Hz in tension-tension at  $R = 0.1$  in an environmental chamber. The environmental chamber permitted evacuation before back filling with ultra high purity H or He gases which were also passed through a liquid nitrogen trap. Crack lengths were measured using macrophotography of the specimen at selected time intervals. For a given crack, the stress intensity range  $\Delta K$  was calculated utilizing a finite width correction factor for an eccentric mode I crack.<sup>13</sup> The inclined cracks all involved a mixture of modes I and II in which case summation of strain energy densities gives an "effective" stress intensity of  $\Delta K = (\Delta K_I^2 + \Delta K_{II}^2)^{1/2}$  from the mode I stress intensity  $\Delta K_I$  and that of mode II,  $\Delta K_{II}$ .

The fatigue crack propagation behavior of the solution-treated polycrystalline specimens (DPH  $\approx 215$ ) and the age hardened Ti-30V alloy single crystals (DPH  $\approx 365$ ) is shown in Figs. 3 and 4. As can be seen, a definite acceleration of the fatigue crack growth rate  $da/dN$  occurs in gaseous hydrogen only when crack propagation takes place in a crystallographic Stage I manner. In this case, propagation occurs in an extended manner on a plane within  $2^\circ$  of the most highly stressed  $\{211\}$  slip plane, the  $(\bar{2}11)$  slip plane in Fig. 2. It is also possible to obtain crystallographic Stage I fatigue in dry He in these age hardened crystals. However, Fig. 4 shows that  $da/dN$  for Stage I fatigue in He is identical in the Paris Law regime with that obtained by testing in laboratory air.\*

As in most other cases involving crystallographic Stage I fatigue on an extended scale, the fracture surfaces appear cleavage-like at low magnifications when Stage I cracking occurs.<sup>1-3,12</sup> At higher magnifications, there is evidence of ductility on the surfaces of the Stage I cracks, especially in the samples tested in He, but there is no evidence of striations. The

\*Data of Salgat and Koss<sup>12</sup> is for Ti-27V single crystals of the same orientation and heat treated also at  $300^\circ\text{C}$  but for 18 hours which results in slightly lower hardness (DPH  $\sim 340$ ) but still predominantly Stage I fatigue crack growth. That data is for samples tested in air at R.F.  $< 30\%$ .

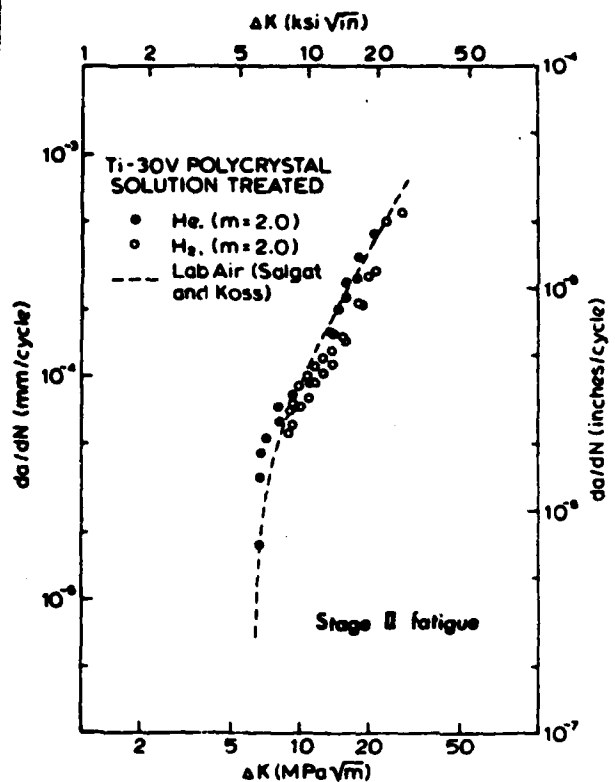


Fig. 3. The fatigue crack propagation rate,  $da/dN$ , as a function of the stress intensity range,  $\Delta K$ , for Ti-30 at. % V polycrystalline samples helium gas quenched from 800°C. Hardness = 215 HB.

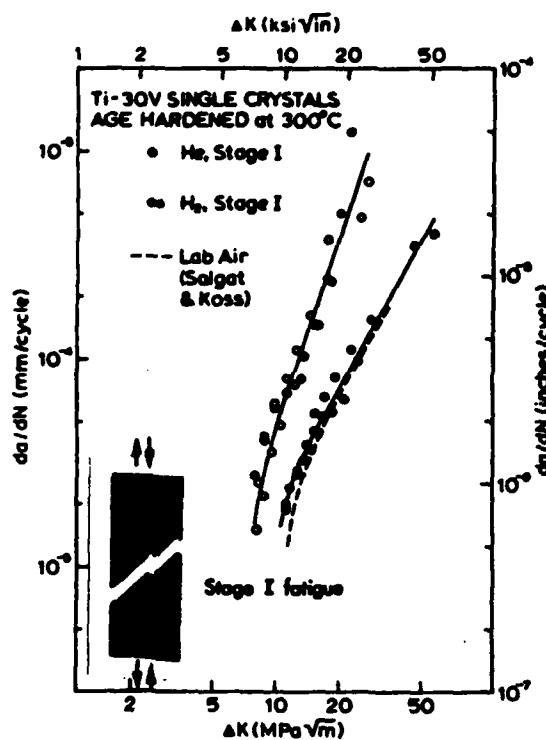


Fig. 4. Stage I fatigue crack propagation rates as a function of stress intensity range for Ti-30 at. % V single crystal specimens quenched from 800°C and aged 52 hours at 300°C. Hardness = 365 HB.

samples tested in  $H_2$  show microcracking on the bottom face of an upward sloping crack, probably due to hydrogen embrittlement and the stress state behind the tip of a mixed mode crack.<sup>14</sup> The Stage II cracks exhibit striations on the fracture surface, the striations being aligned near a  $\langle 110 \rangle$  direction and reflecting propagation by intersecting pairs of  $\{211\}$  slip planes.<sup>15</sup>

#### Correlation of the Fatigue Behavior and the Model

A principal result of this study is that the embrittling effects of gaseous hydrogen occur only when cracking occurs in the age hardened condition along a crystallographic slip band (Stage I fatigue). When the cracking is non-crystallographic (Stage II fatigue), the effect of hydrogen on crack propagation is negligible for the  $\beta$  Ti system studied. We believe that this behavior is a consequence of crack propagation along crystallographic slip bands as described in the first part of this paper. Concerning the hydrogen embrittlement by gaseous hydrogen in the present case, we believe that the key ingredients of this form of cracking are: the relatively large hydrostatic stresses, the location of the maximum in normal stresses being very near the crack-tip, and the presence of planar slip accompanied by a small but significant crack-tip opening displacement normal to the crack faces.

Figure 5 depicts approximately the situation described in the present experiments. It should be noted that Fig. 5 is based on previous calculations<sup>5,6</sup> which are modified for the case of cyclic loading by doubling the yield stress.<sup>16</sup> As is shown in Fig. 5, a substantial hydrostatic stress should exist near the crack-tip,  $\sigma_H^M \approx 6.3 \tau_V^C \approx 2.0$  GPa, where  $\tau_V^C$  is the cyclic shear stress for yielding which is  $\approx 330$  MPa for age-hardened crystals,

assuming  $\tau_y^c \approx \tau_y$ . The location of the maximum stress is also very close to the crack tip ( $x_m \approx .4\mu\text{m}$  @  $\Delta K = 10 \text{ MP}\sqrt{\text{m}}$ ) so that diffusion or sweep-in distances are short. It is noteworthy that these values of  $\sigma_H^m$  and  $x_m$  for the Stage I crack in this bcc alloy do not differ greatly from the magnitude of  $\sigma_H^m$  ( $= 5.3\sigma_y^c \approx 2.6 \text{ GPa}$ , assuming  $\sigma_y^c \approx \sigma_y = 500 \text{ MPa}$ ) and  $x_m = 2\delta$  ( $\approx 1\mu\text{m}$  at  $\Delta K = 10 \text{ MP}\sqrt{\text{m}}$ ) for the Stage II fatigue which shows no hydrogen embrittlement effects. This may be interpreted that either: (a) as suggested previously, planar slip when combined with a small out-of-plane crack opening displacement is critical to hydrogen embrittlement either by causing film rupture or by enhancing dislocation sweep-in of hydrogen onto the coplanar slip bands<sup>17</sup> (which may result in easier slip band decohesion); or (b) that we have underestimated  $\sigma_H^m$  and therefore overestimated  $x_m$  for the Stage I cracks in the age-hardened  $\beta$  Ti alloy. Such errors in  $\sigma_H^m$  and  $x_m$  will occur if a significant amount of cyclic softening occurs causing  $\tau_y^c \ll \tau_y$ ; experimentally cyclic softening does occur in  $\beta$  Ti-V alloys exhibiting planar slip.<sup>18</sup> Thus conditions which are favorable to hydrogen embrittlement exist when crack growth occurs along a crystallographic slip band. These experiments and this analysis do not, however, identify the mechanism by which such embrittlement occurs.

#### Acknowledgements

The authors wish to thank Kwai Chan for helpful comments. We would also like to acknowledge the support of the Air Force Office of Scientific Research through Grant No. 74-2596 and of the Office of Naval Research through Contract No. N00014-76-C-0037.

#### References

1. D. J. Duquette and M. Gell, *Met. Trans.*, 1971, vol. 2, p. 1325.
2. P. E. Irvin and C. J. Beevers, *Met. Trans.*, 1973, vol. 5, p. 391.
3. M. Nageswararao and V. Gerold, *Met. Trans. A*, 1976, vol. 7A, p. 1847.
4. P. Neumann, H. Vehoff and H. Fuhlrott: in *Fracture 1977*, vol. 3, p. 1313, University of Waterloo Press, Waterloo, Canada, 1977.
5. D. A. Koss and K. S. Chan, *Acta Met.* (in print).
6. D. A. Koss and K. S. Chan: in *Acta/Scripta Met. Int. Conf. on Dislocation Modeling of Physical Systems*, Gainesville, FL, 1980 (in print).
7. K. S. Chan and D. A. Koss, *Mat'l. Sci. and Eng.*, 1980, vol. 32, p. 177.
8. G. P. VanderVelde, M. S. Thesis, Michigan Technological Univ., 1979.

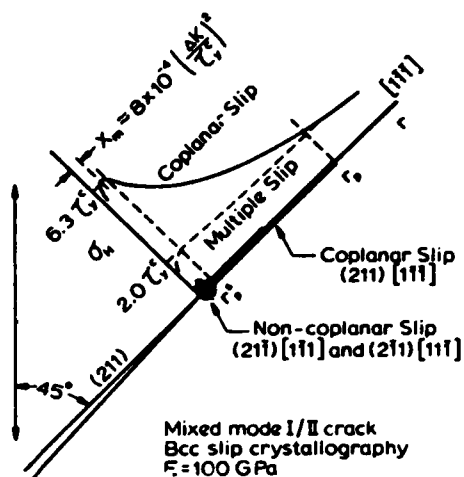


Fig. 3. The approximate distribution of the hydrostatic stress component  $\sigma_H$  as a function of the distance  $x$  ahead of the crack-tip in the plane of the crack. Both coplanar and multiple slip situations are depicted for a  $45^\circ$  mixed mode I/II crack in a material with bcc slip crystallography.

9. J. R. Rice in Stress Corrosion Cracking and Hydrogen Embrittlement, p. 11, NACE, Houston, 1977.
10. N. E. Paton and J. C. Williams in Hydrogen in Metals, p. 409, ASM, Metals Park, 1974.
11. A. Gysler, G. Lutjering and V. Gerold, *Acta Met.*, 1974, vol. 22, p. 901.
12. G. Salgat and D. A. Koss, *Mat'l. Sci. and Eng.*, 1978, vol. 35, p. 263.
13. G. C. Sih in Handbook of Stress Intensity Factors, p. 1.4.3-3, Lehigh Univ. Press, Bethlehem, PA, 1973.
14. M. G. Stout and D. A. Koss, *Met. Trans. A.*, 1978, vol. 9A, p. 835.
15. J. A. Carlson and D. A. Koss, *Acta Met.*, 1978, vol. 26, p. 123.
16. J. Rice in Fatigue Crack Propagation, ASTM STP 415, p. 247, ASTM, Philadelphia, 1967.
17. J. K. Tien, S. V. Nair, and R. R. Jensen, in the Proc. of the Third Int. Conf. on Effect of Hydrogen on Behavior of Materials, Jackson Lake Lodge, Wyoming, Aug. 26-31, 1980.
18. S. B. Chakraborty, T. K. Mukhopadhyay and E. A. Starke, *Acta Met.*, 1978, vol. 26, p. 909.

14 / TR-14

SECURITY CLASSIFICATION OF THIS PAGE (When Data Entered)

REPORT DOCUMENTATION PAGE		READ INSTRUCTIONS BEFORE COMPLETING FORM	
1. REPORT NUMBER No. 14	2. GOVT ACCESSION NO. AD-A089528	3. RECIPIENT'S CATALOG NUMBER	
4. TITLE (and Subtitle) Crack Propagation Along Crystallographic Slip Bands and Hydrogen Embrittlement		5. TYPE OF REPORT & PERIOD COVERED 9 Technical Report	6. PERFORMING ORG. REPORT NUMBER
		7. AUTHOR(s) J. R. Wilcox and D. A. Koss	8. CONTRACT OR GRANT NUMBER(s) N00014-76-C-0037
9. PERFORMING ORGANIZATION NAME AND ADDRESS Department of Metallurgical Engineering Michigan Technological University Houghton, MI 49931		10. PROGRAM ELEMENT, PROJECT, TASK AREA & WORK UNIT NUMBERS	
11. CONTROLLING OFFICE NAME AND ADDRESS Office of Naval Research Dept. of the Navy Arlington, VA 22217		12. REPORT DATE August 1980	
14. MONITORING AGENCY NAME & ADDRESS (if different from Controlling Office)		13. NUMBER OF PAGES	
(12) 11		15. SECURITY CLASS. (of this report) Unclassified	
		15a. DECLASSIFICATION/DOWNGRADING SCHEDULE	
16. DISTRIBUTION STATEMENT (of this Report) Distribution of this document is unlimited.			
17. DISTRIBUTION STATEMENT (of the abstract entered in Block 20, if different from Report)			
18. SUPPLEMENTARY NOTES			
19. KEY WORDS (Continue on reverse side if necessary and identify by block number) Fracture, Stage I Fatigue, Hydrogen Embrittlement, Ti Alloys			
20. ABSTRACT (Continue on reverse side if necessary and identify by block number) The propagation of an inclined crack along a coplanar slip band is examined with regard to the conditions usually associated with hydrogen embrittlement. The analysis shows that large normal stresses are located very near to the crack-tip, despite the mixed mode nature of such cracks. This state of stress, the presence of the planar slip at the crack-tip, and a small but probably significant amount of non-coplanar slip all contribute to a set of conditions which are very favorable to hydrogen embrittlement. In view of (cont'd on back)			

441

SECURITY CLASSIFICATION OF THIS PAGE(When Data Entered)

the analysis, the effect of gaseous environment on the fatigue crack propagation behavior of an age hardenable metastable  $\beta$ -phase Ti-30V alloy has been examined. Tests on both single crystal and polycrystalline specimens show that, consistent with the analysis, gaseous hydrogen accelerates the fatigue crack growth rates only when Stage I fatigue occurs along a crystallographic {112} slip plane.

SECURITY CLASSIFICATION OF THIS PAGE(When Data Entered)